[CANCER RESEARCH 64, 2192–2198, March 15, 2004]

Selective Accumulation of Mature DC-Lamp$^+$ Dendritic Cells in Tumor Sites Is Associated with Efficient T-Cell-Mediated Antitumor Response and Control of Metastatic Dissemination in Melanoma

Mojgan Movassagh,[1] Alain Spatz,[1] Jean Davoust,[1] Serge Lebecque,[2] Pedro Romero,[3] Mikaël Pittet,[3] Donata Rimoldi,[3] Danièle Liénard,[3] Oliver Gugerli,[3] Laurent Ferradini,[4] Caroline Robert,[1] Marie-Françoise Avril,[1] Laurence Zitvogel,[1] and Eric Angevin[1]

[1]Immunology/Institut National de la Santé et de la Recherche Médicale ERM0208 and Immunotherapy Unit, Department of Pathology, Dermatology Unit, Institut Gustave-Roussy, Villejuif, France; [2]Laboratory of Immunological Research, SPRI, Schering-Plough, Dardilly, France; [3]Division of Clinical OncoImmunology, Ludwig Institute for Cancer Research, Lausanne Branch, and Department of Pathology, Centre Hospitalier Universitaire Vaudois, Lausanne, Switzerland; [4]Institut National de la Santé et de la Recherche Médicale U277, Institut Pasteur, Paris, France

ABSTRACT

The clinical relevance of dendritic cells (DCs) at the tumor site remains a matter of debate concerning their role in the generation of effective antitumor immunity in human cancers. We performed a comprehensive immunohistochemical analysis using a panel of DC-specific antibodies on regressing tumor lesions and sentinel lymph nodes (SLNs) in melanoma patients. Here we show in a case report involving spontaneous regression of metastatic melanoma that the accumulation of DC-Lamp$^+$ DCs, clustered with tumor cells and lymphocytes, is associated with local expansion of antigen-specific memory effector CTLs. These findings were extended in a series of 19 melanoma-positive SLNs and demonstrated a significant correlation between the density of DC-Lamp$^+$ DC infiltrates in SLNs with the absence of metastasis in downstream lymph nodes. This study, albeit performed in a limited series of patients, points to a pivotal role of mature DCs in the local expansion of efficient antitumor T-cell-mediated immune responses at the initial sites of metastasis and may have important implications regarding the prognosis, staging, and immunotherapy of melanoma patients.

INTRODUCTION

There is now accumulating evidence that many human cancers elicit antitumor immune responses. Indeed, isolation of specific CTLs has allowed cloning and characterization of genes that encode human tumor-associated antigens in different cancer types (1, 2). Melanoma is considered one of the most immunogenic tumor models because numerous specific and shared tumor antigens have been identified, and tumor-specific CTL responses contributing to spontaneous tumor immunosurveillance have been reported (3). However, few patients receiving the peptide-based vaccines developed to date have shown significant specific immune responses in correlation with clinical regression (4).

Mature dendritic cells (DCs) are the most potent antigen-presenting cells (5) capable of priming tumor-specific T cells, and their use in cancer immunotherapy appears to be a promising way to elicit and expand efficient antitumor immune responses (6, 7). However, little is known about the role of DCs in the natural immunosurveillance of cancer. It is generally postulated that spontaneous immunity against tumor antigens is elicited by DCs maturing in response to various inflammatory signals, but the sites and conditions in which DCs capture and/or encounter tumor antigens remain largely unknown. Indeed, most studies have addressed this question by use of nonspecific antibodies (8), whereas other reports describe the localization and phenotypes of DCs in tumor samples without clinical correlates (9).

Melanoma has become a paradigm for studying the interactions between tumor and host immune cells for the following reasons. First, the primary lesion occurs in the skin, the main residency compartment for Langerhans cells, which have high potential to migrate to skin-draining lymph nodes (LNs; Refs. 10, 11). Second, sentinel LNs (SLNs) are privileged sites of both T-cell priming and initial metastases, the extent of SLN involvement representing an independent predictive factor for survival (12, 13). Third, cutaneous and LN metastases appear to be the tumor sites most sensitive to vaccine-based immunotherapies (6, 14).

Using a panel of antibodies recognizing DC subsets and maturation markers, we addressed the clinical relevance of DC infiltration on regressing tumor lesions and SLNs in melanoma patients. Here we demonstrate, in a case report involving spontaneous regression of metastatic melanoma, dramatic infiltration of DC-Lamp$^+$ DCs in close contact with effector memory Melan-A/Mart-1-specific CTLs *in situ*. In addition, in a series of 19 metastatic SLNs, we also show that the extent of DC-Lamp$^+$ DC infiltration is significantly associated with a high incidence of tumor-free status after lymphadenectomy and a favorable clinical outcome. Altogether, our results strongly suggest that mature DCs play a key role in the local expansion and differentiation of protective tumor-specific immune responses at the first sites of melanoma metastasis.

MATERIALS AND METHODS

Biological Samples

All materials collected in this study were obtained after receipt of informed signed consent, as approved by the Institutional Review Board at the Gustave Roussy Institute and by the Legal Ethical Committee.

Case Report

The patient was a 28-year-old male with an atypical nevus syndrome who in December 2000 developed a right axillar lymphadenopathy corresponding to a melanoma metastasis. The patient reported in the previous months a pigmented nodular lesion in the right arm that had regressed spontaneously. This residual lesion was removed, and a lymphadenectomy in the right axillar basin was performed. Histologically, the cutaneous lesion displayed features typical of regression: absence of associated melanoma cells, a flat epidermis and a fibrotic dermis containing ectasic vessels, heterogeneous melanin pigmentation, and a dense lymphocytic infiltrate. The lymphadenectomy revealed 8 metastatic LNs from a total of 24. After a 10-month disease-free period, a right subclavicular mass developed that corresponded, at surgical examination, to a LN 2 cm in diameter. Histologically, this LN was free of tumor cells and appeared almost completely necrotic with extensive peripheral fibrosis. LN samples were kept frozen for further analyses, and the primary cutaneous site

Received 9/24/03; revised 1/14/04; accepted 1/19/04.

Grant support: CRC/2001-18 grant from Institut Gustave Roussy, the Labelisation by LIGUE Française contre le Cancer, and ARC Foundation.

The costs of publication of this article were defrayed in part by the payment of page charges. This article must therefore be hereby marked *advertisement* in accordance with 18 U.S.C. Section 1734 solely to indicate this fact.

Note: M. Movassagh and A. Spatz contributed equally to this work. J. Davoust is currently at UMR-CNRS 8115, Genethon, 91002 Evry, France.

Requests for reprints: Eric Angevin, M.D. Ph.D, Unité d'Immunologie/INSERM ERM0208, Département de Biologie Clinique, Institut Gustave Roussy, 94805 Villejuif Cedex, France. Phone: (33) 1 42 11 50 35; Fax: (33) 1 42 11 60 94; E-mail: angevin@igr.fr.

was paraffin-embedded only. This patient remains disease-free 34 months after diagnosis without any adjuvant therapy.

Series of 19 Melanoma-Positive SLNs

All patients underwent surgical SLN resection at the time of or a few weeks after excision of the primary cutaneous melanoma, according to the recommended procedures (12). For this study, we selected a consecutive series of 19 patients with a melanoma-positive SLNs followed in our institution between June 1999 and March 2002. A few weeks after the SLN procedure, all underwent a regional completion lymphadenectomy to detect metastatic extensions in non-SLNs. The materials used consisted of paraffin-embedded sections from recorded paired SLN and non-SLN samples.

Characterization of Melan-A/Mart-1-Specific CTLs from Peripheral Blood

Immunophenotyping Using Phycoerythrin (PE)-Labeled HLA-A*0201/Peptide Tetramer Complexes. HLA-A*0201/Melan-A/Mart-1_{26-35} A27L analog (ELAGIGILTV) and control HLA-A*0201/HIVgag$_{77-85}$ (SLYNTVATL) were synthesized as described previously (15). Total peripheral blood mononuclear cells or immunopurified $CD8^+$ T cells, obtained after magnetic cell sorting with a MiniMACS device ($CD8^+$ T Cell Isolation Kit; Miltenyi Biotec, Bergisch Gladbach, Germany), were stained with the PE-labeled tetramers (5 nM) at room temperature for 45 min in PBS containing 2% BSA, washed once, stained for cell surface differentiation antigens with monoclonal antibodies (mAbs) for 30 min at 4°C, washed again, and analyzed by flow cytometry. Conjugated anti-CD3, -CD8, and -CD45RA mAbs were purchased from BD Biosciences (Le Pont de Claix, France), and anti-TCRVβ2 and -TCRVβ3 were purchased from Beckman Coulter (Villepinte, France). Samples were also incubated with anti-CCR7 rat IgG2a mAb 3D12 (kindly provided by M. Lipp, Berlin, Germany) for 30 min at 4°C, washed, and additionally stained with an antigen-presenting-cell-labeled goat antirat IgM+IgG (Southern Biotechnology, Birmingham, AL). Fluorescent isotype-matched mAbs were used as controls. Direct *ex vivo* analysis was performed after acquisition of $>10^6$ events on a FACSCalibur (BD Biosciences) with Cellquest software.

Sorting, Cloning, Expansion, and Characterization of Anti-Melan-A/Mart-1 CTLs. $CD3^+CD8^+$HLA-A*0201/Melan-A/Mart-$1_{26-35}{}^+$ cells were sorted by flow cytometry with FACS Vantage (BD Biosciences) and cultured in V-bottomed 96-well plates either in bulk or after direct cloning in limiting dilution on feeder cells consisting in irradiated allogeneic peripheral blood mononuclear cells, EBV-transformed LAZ509 B cells, and MEL-FON tumor cells, a HLA-$A2^+$ melanoma tumor cell line expressing the Melan-A/Mart-1 antigen (15). Growing clonal colonies were expanded at 37°C and 5% CO_2 in RPMI 1640 (Life Technologies, Inc., Paisley, United Kingdom) supplemented with 10% human AB serum (Institut Jacques Boy, Reims, France), 50 IU/ml recombinant human interleukin-2 (Proleukin; Chiron, Rattingen, Germany), and 3% T-cell growth factor, a supernatant from phytohemagglutinin/phorbol 12-myristate 13-acetate-allostimulated T cells. T-cell clones were characterized for immunophenotype by use of HLA-A*0201/Melan-A/Mart-1_{26-35} tetramers and mAbs directed against CD3 and CD8 and by TCR-Vβ repertoire analysis with a panel of 21 anti-BV mAbs (IOTest β Mark; Beckman Coulter Immunotech, Marseille, France), and for cytotoxic activity in a standard 4-h ^{51}Cr-release assay against MEL-FON tumor cells and Transporter associated with Antigen Processing (TAP)-deficient EBV-transformed T2 cells loaded with 10 μg/ml Melan-A/Mart-1_{26-35} synthetic peptide. IFN-γ secretion in response to the same targets was also assessed by use of the high-affinity capture matrix assay according to the manufacturer's instructions (IFN-γ secretion assay; Miltenyi Biotec).

In Situ Tetramer Staining Analyses

Tissue samples were snap-frozen immediately after collection and cryopreserved in liquid nitrogen until use. Serial multiple 10-μm cryostat tissue sections were used for *in situ* tetramer staining. To block nonspecific binding sites, tissue sections were first recovered with 200 μl of 1× PBS containing 0.5% BSA and 10% FCS for 15 min at room temperature. After elimination of the buffer, PE-labeled HLA-A*0201/Melan-A/Mart-1_{26-35} or peptide-irrelevant tetramer complexes were incubated at 2.6 μg/ml for 45 min at room temperature in a dark humidified atmosphere. The sections were washed with PBS and incubated with direct fluorescence or biotin-conjugated mAbs (anti-CD3, -CD8, -TCRVβ2, and -TCRVβ3) for an additional 30 min at 4°C. For triple staining, the biotin-coupled antibody was detected with streptavidin-Cy5.5 conjugate. After washing, sections were fixed with PBS-buffered 1% formaldehyde for 15 min at room temperature, mounted in antifading medium, and covered with a coverslip. Slide examination and micrography were performed with a fluorescence microscope (DMRXA; Leica, Weitzlar, Germany), and/or slides were evaluated with a Leica SP1 confocal microscopy system equipped with an Ar/Kr laser for the 488 and 568 nm lines and a HeNe633 laser (Leica Laser Technik; Mannheim, Germany) to excite the Cy5.5 label. Simultaneous acquisition of signals for the FITC-, PE-, and Cy5.5-labeled antibodies was performed at low illuminating laser power and with spectrophotometer-based separation of the fluorescence emissions. The fields of interest were selected on the basis of CD8- or TCRVβ2-FITC-labeled infiltrates to avoid bias in scoring of tetramer-PE staining before confocal image acquisition.

Immunohistochemistry of Infiltrating T Cells and Antigen-Presenting Cells

Sections 4-μm thick were prepared on glass slides from paraffin-embedded formaldehyde-fixed material and were deparaffinized and rehydrated. For all antibodies except for anti-CD123, -CCR7, and -CD68, slides were pretreated in sodium citrate at 68°C (pH 6) for 20 min. After a blocking step (Blocking agent, Ultra-tech HRP kit; Beckman-Coulter Immunotech), slides were incubated with the primary antibodies at the following dilutions: 1:1 for anti-CD1a and anti-CD68 (Immunotech); 1:20 for anti-MIP3α/CCL20 (Schering-Plough, Dardilly, France); 1:50 for anti-CD3, anti-CD4 (Dako, Trappes, France), and anti-MIP3β/CCL21 (R&D Systems, Abingdon, United Kingdom); 1:60 for anti-p55 (Dako); 1:100 for anti-CD8 (Dako) and TIA-1 (Beckman Coulter); 1:200 for anti-Langerin (Schering-Plough) and anti-CCR7 (BD PharMingen); 1:300 for anti-DC Lamp and anti-CD123 (Schering-Plough); and 1:500 for anti-CCR6 and anti-6CKine/CCL19 (R&D Systems) for 1 h at room temperature, followed by incubation with secondary antibodies and detection (Ultra-tech HRP kit). The slides were examined by two independent observers. Semiquantitative evaluation of DC-$Lamp^+$ DC infiltration was made as follow: (*a*) the slide was examined at intermediate magnification (×100) to select the three areas containing the maximum number of DC-$Lamp^+$ DCs; (*b*) the number of DC-$Lamp^+$ cells per mm^2 was then counted at high magnification (×400) in 3-mm^2 sections per hot spot; (*c*) the final count used for DC-Lamp quantitative evaluation was the average number of the nine countings made on the slide. Statistical analyses comparing the groups according to DC-$Lamp^+$ DC infiltration used Fisher's exact method, and statistically significant differences were given at 95% confidence.

RESULTS AND DISCUSSION

Evidence for Peripheral Memory Melan-A/Mart-1-Specific CTLs Recognizing Melanoma. We report here the case of a young HLA-A*0201-positive patient presenting with a completely regressive primary cutaneous melanoma associated with regressing regional metastatic LNs. Postulating that this favorable clinical outcome might have resulted from an efficient antitumor immune response, we thus focused this study on the peripheral CTL response directed against the Melan-A/Mart-1 tumor antigen strongly expressed at the site of the first metastatic LNs, as assessed by reverse transcription-PCR (data not shown). As shown in Fig. 1*A*, direct *ex vivo* staining of peripheral $CD3^+CD8^+$ T lymphocytes with HLA-A*0201/Mart-1_{26-35} tetramers revealed 0.15% specific T lymphocytes, which produced four $tetramer^+$ T-cell clones. Two expressed TCR-V$\beta2^+$ with specificities for BV2J2.6 and BV2J2.7 gene segments, one expressed V$\beta3^+$ (BV3J1.5), and one expressed V$\beta13^+$ (BV13; Fig. 1*B*). All of these CTL clones recognized not only TAP-deficient T2 cells pulsed with Melan-A/Mart-1_{26-35} peptide, but also the naturally processed Melan-A/Mart-1 antigen presented by the HLA-$A2^+$ MEL-FON melanoma cell line, as assessed by cytotoxicity (Fig. 1*B*) and IFN-γ secretion assays (data not shown). Interestingly, half-maximal lysis of peptide-

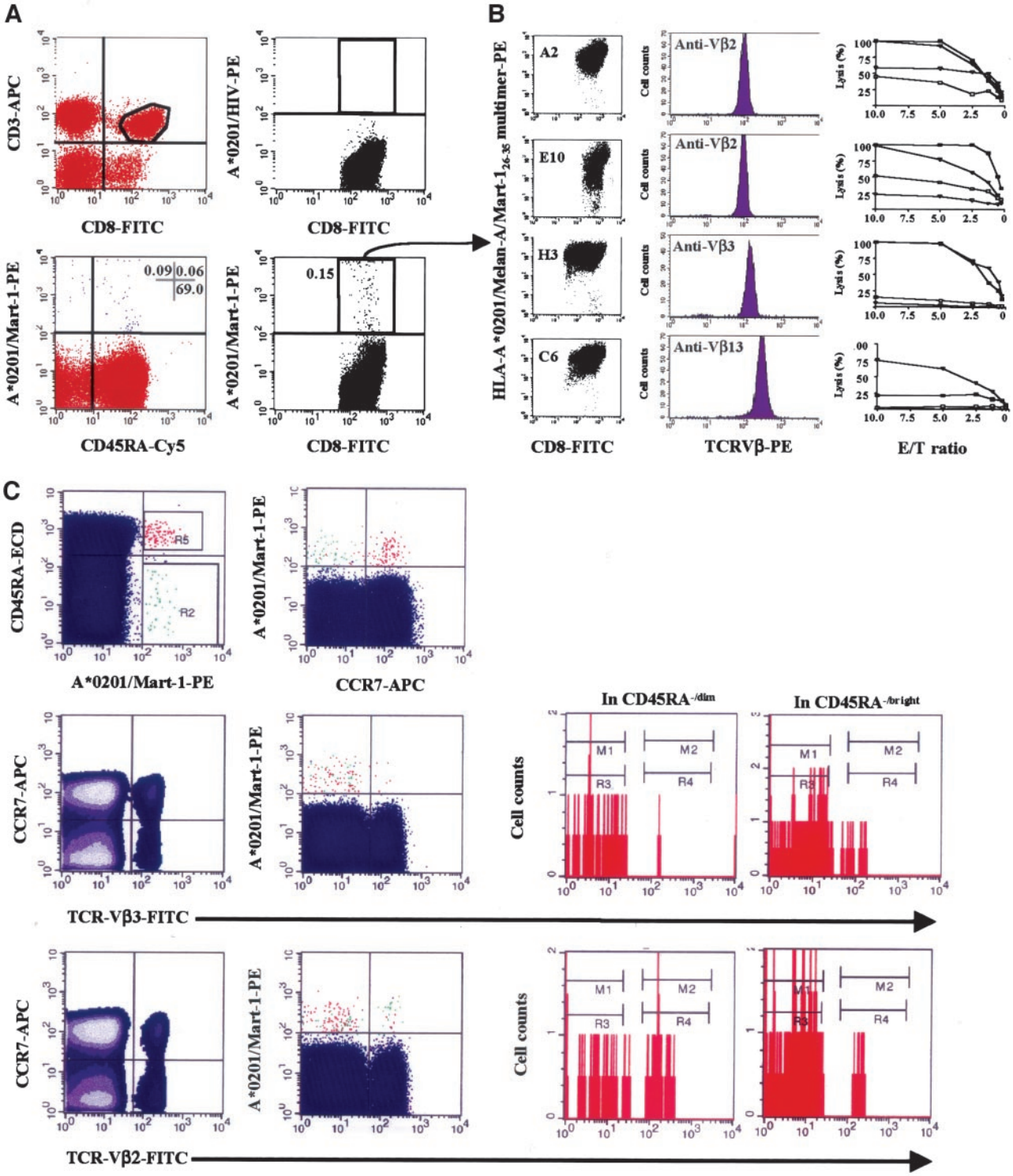

Fig. 1. Circulating HLA-A*0201/Mart-1_{26-35}^{+} CD8^{+} T cells contain a melanoma-reactive memory Vβ2^{+} T-cell subpopulation. *A*, flow cytometric analysis of Melan-A/Mart-1-specific T cells in peripheral blood mononuclear cells. *B*, sorting of CD3^{+}CD8^{+}HLA-A*0201/Mart-1_{26-35}^{+} cells and isolation after limiting dilution cultures of four CTL clones characterized for TCRVβ usage by use of specific monoclonal antibodies and for cytolytic activity against the HLA-A2^{+}/Mart-1^{+} MEL-FON tumor cells (■) inhibited by the anti-MHC class I W6.32 monoclonal antibody (□) and T2 cells pulsed with Mart-1_{26-35} or irrelevant peptides (▲ and △, respectively). *C*, analysis of Melan-A/Mart-1-specific T cells in immunopurified CD8^{+} peripheral T cells according to CD45RA and CCR7 phenotyping. Although a majority of HLA-A*0201/Mart-1_{26-35}^{+} T cells in the CD8^{+} cells, as well as in the Vβ3^{+} T-cell subset, displayed a naive CD45RA^{+}CCR7^{+} (*red dots*) phenotype, CD45RA$^{-/dim}$/CCR7^{-} (*green dots*) memory cells were preferentially found in the Vβ2^{+} T-cell subpopulation. PE, phycoerythrin; ECD, phycoerythrin-Texas Red; APC, allophycocyanin.

pulsed T2 cells was observed with peptide concentrations ranging from 5×10^{-9} to 5×10^{-10} M, demonstrating the high T-cell receptor (TCR) avidity of these clones (data not shown), which were all brightly stained with the tetramers (Fig. 1*A*). Such high-avidity TCRs have been reported to be expressed by melanoma-reactive CTLs, whereas CD8^{+} T cells with impaired proliferative and effectors functions mostly display low-avidity TCRs (16).

Naive central and effector memory T lymphocytes can now be

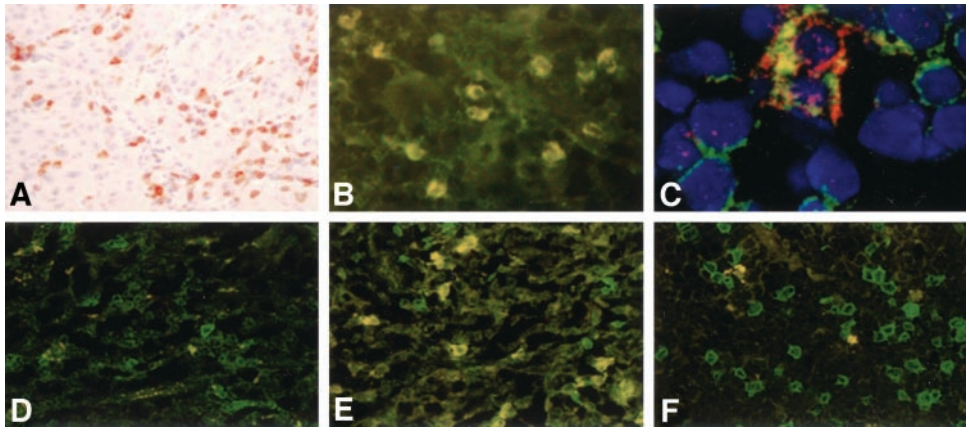

Fig. 2. *In situ* characterization of Melan-A/Mart-1-specific CD8 T cells in a metastatic lymph node (LN) draining a regressive melanoma. *A–E*, Metastatic LNs; *F*, nonmetastatic LN draining the primary tumor in the same patient. *A*, anti-TIA-1 immunostaining reveals numerous positive lymphocytes in the vicinity of tumor cells. *B–F*, *in situ* tetramer staining. *B* and *C*, double staining with FITC-labeled anti-CD8 and phycoerythrin (PE)-labeled HLA-A*0201/Mart-1_{26-35} tetramer; *D*, double staining with FITC-labeled anti-TCRVβ2 and PE-labeled HIVgag$_{77-85}$ tetramer as negative control; *E* and *F*, double staining with FITC-labeled anti-TCRVβ2 and PE-labeled HLA-A*0201/Mart-1_{26-35} tetramer. Significant numbers of anti-Melan-A/Mart-1-specific CD8$^+$ or TCRVβ2$^+$ T cells (*yellow stained*) were reproducibly detected infiltrating the tumor area in the metastatic LN (*B*, *C*, and *E*) but not in the nonmetastatic LN (*F*).

discriminated to delineate the stages of lymphocyte differentiation after antigen encounter and stimulation *in vivo* (17). To characterize the differentiation status of the HLA-A*0201/Mart-1_{26-35} tetramer$^+$ T lymphocytes found in this patient, we analyzed peripheral blood mononuclear cell-derived CD8$^+$ T lymphocytes by four-color immunophenotyping using anti-CD45RA, -CCR7, and -TCRVβ mAbs. As shown in Fig. 1*C*, we confirmed the predominance of naive (CD45RA^{bright}CCR7$^+$) over memory (CD45RA$^{-/dim}$CCR7$^-$) anti-Melan-A/Mart-1 T cells (18, 19). However, although the majority of tetramer$^+$Vβ3$^+$CD8$^+$ T cells appeared to be naive, most tetramer$^+$Vβ2$^+$ cells displayed a memory phenotype (Fig. 1*C*). We thus addressed the relevance of such a melanoma-reactive memory T-cell response with high-avidity TCRVβ2$^+$ cells in the spontaneously regressing lesions.

***In Situ* Characterization of Tumor-Infiltrating Melan-A/Mart-1-Specific CTLs.** The lymphocytic infiltrate of the metastatic LNs contained a majority of CD3$^+$CD8$^+$ lymphocytes displaying a dominant Vβ2 specificity (data not shown). Importantly, a high proportion of lymphocytes were stained with the TIA-1 mAb, which recognizes perforin/granzyme-containing granules that are preferentially associated with memory/effector cytotoxic functions (Fig. 2*A*). To determine the Melan-A/Mart-1 specificity of tumor-infiltrating CTLs in the first metastatic LN, we performed a double staining with PE-labeled HLA-A*0201/Mart-1_{26-35} tetramer and FITC-labeled anti-CD8 or anti-Vβ2 mAbs. We observed significant numbers of tetramer$^+$CD8$^+$ T lymphocytes (*e.g.*, >10 cells at high magnification) in the tumor areas (Fig. 2, *B* and *C*), approximately half of which were Vβ2$^+$ cells (Fig. 2*E*). However, a more precise quantification of specific T cells by flow cytometry analysis could not be performed because fresh LN fragments were not available at the time of lymphadenectomy. The specificity of tetramer staining was assessed with a peptide-irrelevant PE-labeled HLA-A*0201/HIVgag$_{77-85}$ tetramer on serial sections of the same LN (Fig. 2*D*) and with the relevant PE-labeled HLA-A*0201/Mart-1_{26-35} tetramer on a tumor-free alternative LN from the same axillary area (Fig. 2*F*). Confocal microscopy revealed in double-positive cells an overlay of FITC and PE labeling concordant with the colocalization of TCR signals obtained with tetramers and anti-TCR mAbs (Fig. 2*E*). Of note, tetramer staining was frequently polarized toward the T-cell membrane directly in contact with adjacent tumor cells with occasional intracellular vesicles, suggesting capping and/or recycling of TCR-containing vesicles. These features may also correspond to dense accumulation in lipid rafts and engagement of TCRs, an important process for T-cell activation; lipid raft integrity is also required for efficient MHC class I tetramer binding (20).

Although direct visualization by use of fluorescent MHC class I/peptide complexes of antigen-specific T cells on fresh tissue sections has already been reported (21, 22), the clinical application of this technique to human tumors remains limited by the very low frequency of infiltrating CTLs that are specific for a given epitope. Here we demonstrate, however, that such *in situ* tetramer staining can be applied successfully on informative sites, such as a metastatic LN draining a spontaneously regressive primary melanoma. The close contact of Melan-A/Mart-1-specific T lymphocytes with tumor cells suggests their active role in the efficient natural immunosurveillance ongoing in this patient.

Accumulation of Maturing DCs Interacting with Tumor Cells in LN T-Cell-Rich Areas. The availability of a panel of mAbs directed against DC surface molecules enabled staining of paraffin-embedded tissue sections and allowed us to characterize the infiltrating DCs in the different samples collected from this patient. We first examined two Langerhans cell markers, CD1a and the lectin Langerin/CD207, which are both expressed by immature Langerhans cells. As for the noninvaded adjacent skin, numerous intradermal CD1a$^+$ and Langerin$^+$ cells were detected in the epidermis of the primary regressing cutaneous lesion (data not shown), but very few were observed in the draining metastatic LNs. Such findings contrasted with the detection of significant numbers of CD1a$^+$ and Langerin$^+$ cells in the subcapsular areas of normal LNs collected from other donors (data not shown). In addition, in contrast to what is also seen in normal LNs, we found no CD123/IL-3Rα^+ plasmacytoid DCs in the LNs of our patient (not shown).

We also examined the expression of the actin-bundling protein p55/fascin and the lysosomal protein DC-Lamp, both of which are associated with a mature DC phenotype. In the metastatic LN (Fig. 3*A*) as well as in the residual lymphocytic regions of the necrotic LN (not shown), we observed dense infiltration of p55$^+$/DC-Lamp$^+$ double-positive cells within the T-cell-rich regions and peritumoral areas, which contrasted with the scattered and mostly subcapsular localization in a nonmetastatic LN (Fig. 3*B*). These cells exhibited the typical morphology of "mature" DCs and were surrounded by T lymphocytes forming clusters (Fig. 3, *C*, *E*, and *G*) that have been described as characteristic of ongoing immune reactions and have been observed at the periphery of human breast tumor cell clusters (9). DC-Lamp$^+$ (not shown) or p55$^+$ DCs (Fig. 3*G*) frequently also accumulated around neomicrovessels within tumor areas. We made similar observations in the primary skin site, where p55$^+$ DCs were often surrounded by lymphocytes in the regression area but not in the normal adjacent dermis (not shown), suggesting local recruitment and/or differentiation of DC precursors from the peripheral blood. Interestingly, in a metastatic LN (Fig. 3*C*), the cellular localization of DC-Lamp was diffuse, including staining of peripheral dendrites, in contrast to that observed in a nonmetastatic LN (Fig. 3*D*), in which the

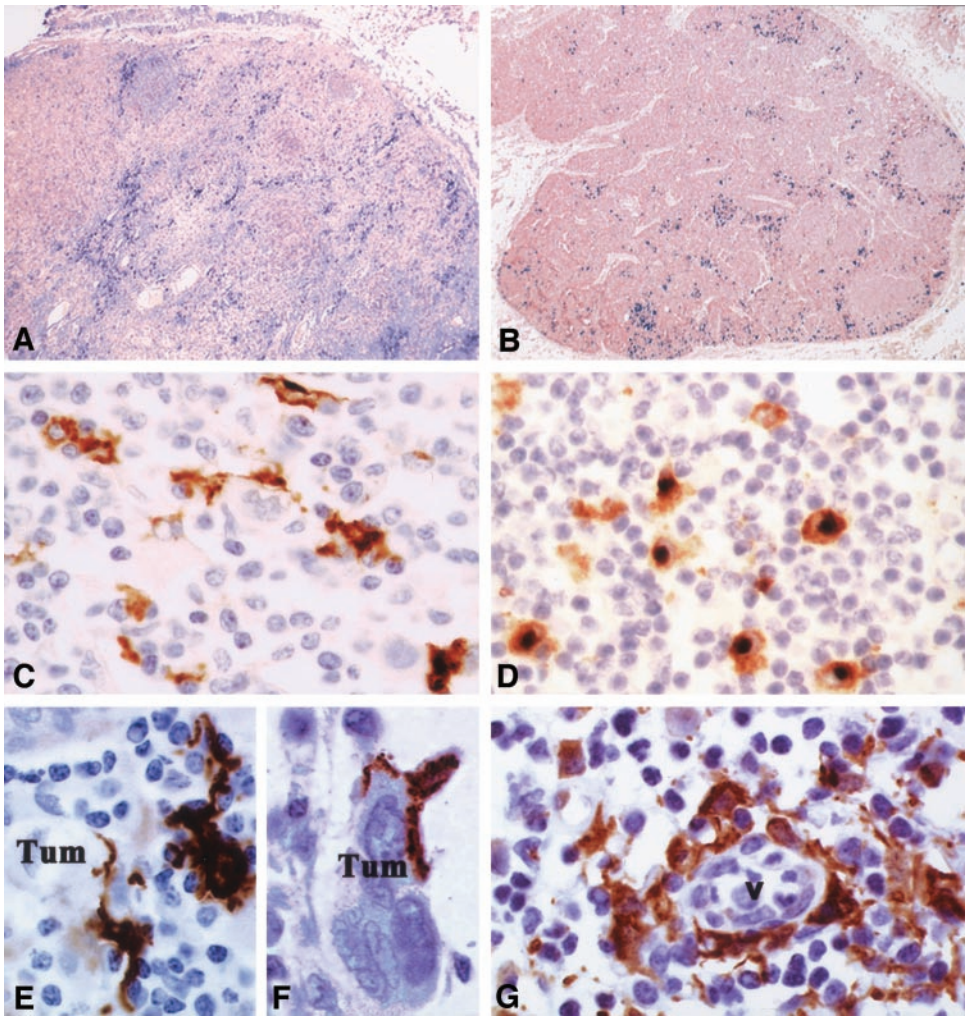

Fig. 3. Accumulation of DC-Lamp$^+$ mature dendritic cells (DCs) interacting with tumor cells in T-cell-rich areas of metastatic lymph node (LN). *A, C, E–G,* metastatic LN; *B* and *D,* nonmetastatic adjacent LN. *A* and *B,* immunostaining with anti-p55 and anti-DC-Lamp antibodies (Schering-Plough). In the metastatic LN (*A*), DC-Lamp$^+$ mature DCs accumulate throughout the whole node with a predominance in T-cell-rich regions, whereas in the nonmetastatic LN (*B*) DC-Lamp$^+$ DCs are located mainly in the subcapsular and perifollicular areas. *C* and *D,* immunohistochemistry with DC-Lamp antibody displays a diffuse and peripheral staining of dendrites in the metastatic LN (*C*) that contrasts with juxtanuclear dot-like staining in nonmetastatic LN (*D*). *E* and *F,* representative clusters of DC-Lamp$^+$ DCs in close contact with melanoma tumor cells (*Tum*) and lymphocytes. *G,* in some areas, p55$^+$ DCs accumulate around blood vessels.

DC-Lamp staining appeared mostly concentrated in a "dot-like" juxtanuclear region of the cells. Considering that DC-Lamp has previously been reported to accumulate in juxtanuclear late lysosomal compartments during maturation (23), these findings suggest that an efficient immune response is more likely associated with a maturing DC phenotype rather than with a fully mature differentiation stage. Although the function of DC-Lamp has not been elucidated, our results indicate that its subcellular localization and/or its abundance on DC membranes in close apposition with tumor cells could be beneficial for tumor antigen capture and presentation or is associated with the presence of highly active antigen-presenting cells.

The scenario involving DCs, T lymphocytes, nonspecific effector cells such as macrophages, and tumor cells orchestrated to elicit an effective immune response *in situ* remained elusive. Nonetheless, we frequently observed veiled dendritic p55$^+$ or DC-Lamp$^+$ projections tightly apposed to tumor cells (Fig. 3, *E* and *F*), reminiscent of data from experimental *in vitro* systems in which DCs ingested tumor cell bodies and processed tumor-associated antigens to elicit specific immune responses (10). Because these DCs also interacted with several surrounding lymphocytes, one can postulate that such interactions may trigger *in situ* activation, expansion, and effector functions of antigen-specific T cells, culminating, as in this patient, in tumor regression.

Expression of CCR6/CCR7 and Their Ligands in the Metastatic LN. Considering their critical role in DC chemoattraction, we assessed the expression of the CC chemokine receptors (CCR) CCR6 and CCR7 and their respective ligands, MIP-3α/LARC (CCL20), 6CKine/SLC (CCL19), and MIP-3β/ELC (CCL21). In the metastatic LN, we found that CCR6 was expressed predominantly within tumor areas by cells exhibiting a dendritic morphology (Fig. 4*A*). Accordingly and as described previously (9), tumor cells and macrophages strongly expressed the CCR6 ligand CCL20 and clearly colocalized with CCR6$^+$ DCs (Fig. 4*B*). CCR7 was expressed by a few cells in tumor areas, *i.e.*, tumor cells and lymphocytes, but not by infiltrating DCs (Fig. 4*C*). In contrast, large dendrite-shaped CCR7^{bright} cells were detected occasionally in the T-cell-rich areas without tumor cell infiltration (Fig. 4*D*), and the CCR7 ligands CCL19 and CCL21 were slightly positive on DCs and stromal and endothelial cells of microvessels (not shown). During their migration from blood to peripheral tissues, CCR6$^+$ DC precursors appear to be attracted by a CCL20 gradient that is established by local inflammation (5, 10, 24). Peripheral immature DCs may then undergo a maturation process characterized by several modifications, including the reciprocal loss of CCR6 and acquisition of CCR7, with resulting responsiveness to CCL19/CCL21 (24). However, whether DC chemoattraction to LNs and DC maturation are concomitant processes remains controversial (25, 26). As reported in psoriasis (27), rheumatoid arthritis (28), and in some reports, cancer (9, 29), our findings of dominant CCR6/CCL20 expression suggest that the tumor-invaded LN should be considered as an inflammatory site rather than a typical lymphoid organ. Therefore, in this metastatic LN, maturing DCs might indeed display significant heterogeneity regarding expression of CCR recep-

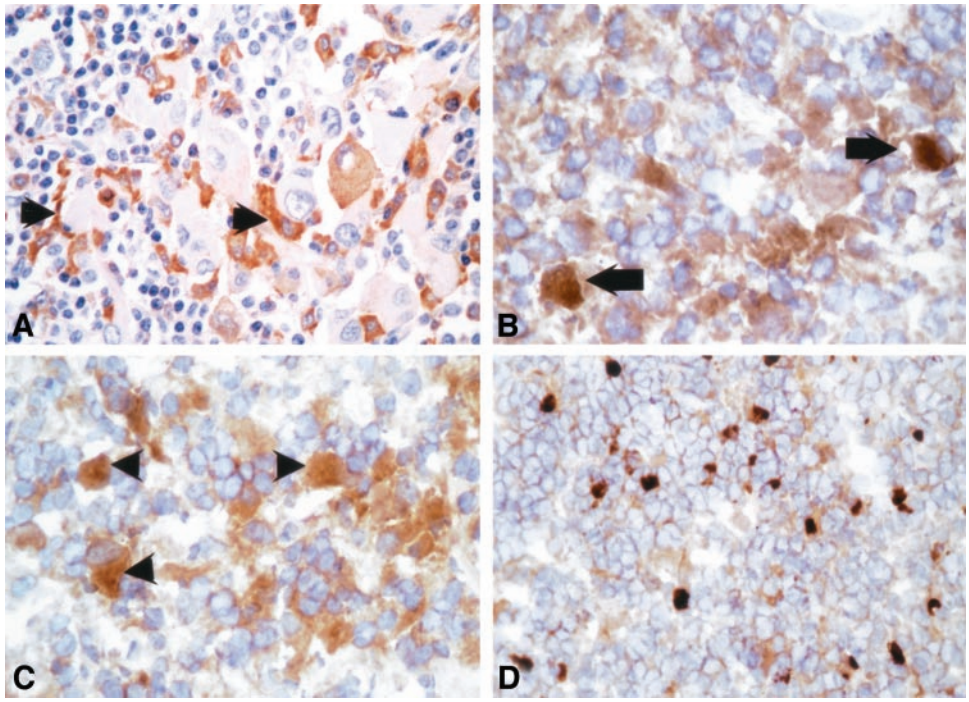

Fig. 4. Immunohistochemical staining of CCR6/CCL20 and CCR7 in the metastatic lymph node. *A*, CCR6 is preferentially expressed in cells with a dendritic morphology (*arrows*) in the immediate vicinity of tumor cells. *B*, tumor cells and macrophages (*arrows*) strongly express CCL20 in tumor areas. *C* and *D*, anti-CCR7 immunostaining. In tumor areas, CCR7 is expressed by various cell types, including tumor cells (*C*; *arrows*), but not by infiltrating dendritic cells, whereas large dendritic-shaped CCR7^{bright} cells are found only in tumor-free T-cell-rich regions (*D*).

tors and could even transiently coexpress CCR6 and CCR7 in an intermediate stage of maturation, as has been reported recently (30). Altogether, these data point to a potential role of MIP3α/CCL20 in the local recruitment of DCs in metastatic LNs.

Density of DC-Lamp$^+$ DCs in Melanoma-Positive SLNs Is Inversely Correlated with Metastasis in Downstream LNs. The most striking observation associated with spontaneous tumor regression in this case report was the dramatic accumulation of DC-Lamp$^+$ mature DCs in metastatic LNs. However, because this finding was based on one informative patient, we assessed the presence of mature DCs in a series of 19 additional melanoma-positive SLNs. Because SLNs are identified as the first site of melanoma metastases, we postulated that the extent of mature DC infiltration may dictate the induction of efficient local antitumor immune responses. The following parameters were thus evaluated by two independent observers: (*a*) semiquantitative evaluation of the absolute number of DCs counted at sites of highest SLN infiltration, which led to the identification of two groups of patients: SLN/DC-Lamp^{low} (+ or ++, *i.e.*, <100 or 100–300 DC-Lamp$^+$/mm^2, respectively; $n = 11$) and SLN/DC-Lamp^{high} (+++, *i.e.*, >300 DC-Lamp$^+$/mm^2; $n = 8$); (*b*) the aspect of DC-Lamp staining, *i.e.*, dendritic or dot-like, that could correspond to a maturing or fully mature phenotype, respectively; (*c*) tumor infiltration of DC-Lamp$^+$ cells and evidence for clusters of DC-Lamp$^+$ cells with tumor cells and lymphocytes (in 10 of the 19 melanoma-positive SLNs in which tumor cells could be visualized). The results are summarized in Table 1. In the SLN/DC-Lamp^{low} group, DC-Lamp$^+$ cells displayed a predominant dot-like lysosomal staining, whereas in the SLN/DC-Lamp^{high} group, DC-lamp$^+$ cells displayed a predominant dendritic staining ($P = 0.019$) and an increased frequency of tumor infiltration and DC clustering, as mentioned in the case report. Furthermore, there was a striking inverse correlation between the density of DC-Lamp infiltrates and the occurrence of at least one melanoma-positive non-SLN in the subsequent regional completion lymphadenectomy performed a few weeks after the SLN resection. Seven of 11 patients in the SLN/DC-Lamp^{low} group had at least one metastatic non-SLN, in contrast to none of 8 patients in the SLN/DC-Lamp^{high} group ($P = 0.013$). We will attempt to validate this correlation between the presence of mature DCs in the initial metastatic lesion and the absence of secondary metastatic spread in a comprehensive multicenter study aimed at evaluating the prognostic value of DC-Lamp and other dendritic cell markers in disease-free and overall survival of a large cohort of patients with primary cutaneous melanoma.

Our data strongly suggest that mature DC-Lamp-expressing DCs play a pivotal role in melanoma immunosurveillance at the initial site of metastasis and in eliciting the generation of an effective antitumor

Table 1 *Density of DC-Lamp$^+$ dendritic cells in melanoma-positive sentinel lymph nodes is correlated with the absence of metastasis in downstream lymph nodes*

Parameters analyzed	SLN[a]/DC-Lamp^{low}	SLN/DC-Lamp^{high}	Significance[b]
Density (DC-Lamp$^+$ cells/mm^2)	<300	>300	
Patients (n)	11	8	
Morphology of DC-Lamp staining (n)			
Dendritic	3	7	
Dot-like	8	1	$P = 0.0198$
Infiltration of tumor by DC-Lamp$^+$ cells[c] (n)			
Yes	2/6	3/4	NS
Clusters of DCs/tumor cells/lymphocytes	1/6	2/4	NS
No	4/6	1/4	NS
Patients with metastatic non-SLNs in lymphadenectomy (n)	7	0	$P = 0.0128$

[a] SLN, sentinel lymph node; NS, not significant; DC, dendritic cell.
[b] Using the Fisher's exact test.
[c] Tumor areas evidenced on the slides of 10 positive sentinel lymph nodes used for DC-Lamp immunohistochemistry.

response with local T-cell activation/expansion. These observations may also have implications regarding the identification of new prognostic groups of melanoma patients with high infiltration of DC-Lamp$^+$ DCs in SLNs, in whom immunotherapy in early adjuvant settings could be successful.

ACKNOWLEDGMENTS

We gratefully acknowledge Christophe Le Boullaire and Valérie Vélasco for excellent technical assistance, Patrick Bruneval for constant support in confocal microscopy, and Yann Lecluse and Pascal Batard for flow cytometry cell-sorting experiments.

REFERENCES

1. Boon T, Coulie PG, Van den Eynde EB. Tumor antigens recognized by T cells. Immunol Today 1997;18:267–8.
2. Rosenberg SA. A new era for cancer immunotherapy based on the genes that encode cancer antigens. Immunity 1999;10:281–7.
3. Mackensen A, Carcelain G, Viel S, et al. Direct evidence to support the immunosurveillance concept in a human regressive melanoma. J Clin Investig 1994;93:1397–402.
4. Coulie PG, Bruggen P. T-cell responses of vaccinated cancer patients. Curr Opin Immunol 2003;15:131–7.
5. Banchereau J, Steinman RM. Dendritic cells and the control of immunity. Nature (Lond.) 1998;392:245–52.
6. Nestle FO, Alijagic S, Gilliet M, et al. Vaccination of melanoma patients with peptide- or tumor lysate-pulsed dendritic cells. Nat Med 1998;4:328–32.
7. Schuler-Thurner B, Schultz ES, Berger TG, et al. Rapid induction of tumor-specific type 1 T helper cells in metastatic melanoma patients by vaccination with mature, cryopreserved, peptide- loaded monocyte-derived dendritic cells. J Exp Med 2002; 195:1279–88.
8. Lana AM, Wen DR, Cochran AJ. The morphology, immunophenotype and distribution of paracortical dendritic leucocytes in lymph nodes regional to cutaneous melanoma. Melanoma Res 2001;11:401–10.
9. Bell D, Chomarat P, Broyles D, et al. In breast carcinoma tissue, immature dendritic cells reside within the tumor, whereas mature dendritic cells are located in peritumoral areas. J Exp Med 1999;190:1417–26.
10. Banchereau J, Briere F, Caux C, et al. Immunobiology of dendritic cells. Annu Rev Immunol 2000;18:767–811.
11. Geissmann F, Dieu-Nosjean MC, Dezutter C, et al. Accumulation of immature Langerhans cells in human lymph nodes draining chronically inflamed skin. J Exp Med 2002;196:417–30.
12. Cochran AJ, Huang RR, Guo J, Wen DR. Current practice and future directions in pathology and laboratory evaluation of the sentinel node. Ann Surg Oncol 2001;8: 13S–7S.
13. Starz H, Balda BR, Kramer KU, Buchels H, Wang H. A micromorphometry-based concept for routine classification of sentinel lymph node metastases and its clinical relevance for patients with melanoma. Cancer 2001;91:2110–21.
14. Marchand M, van Baren N, Weynants P, et al. Tumor regressions observed in patients with metastatic melanoma treated with an antigenic peptide encoded by gene MAGE-3 and presented by HLA-A1. Int J Cancer 1999;80:219–30.
15. Motta I, Andre F, Lim A, et al. Cross-presentation by dendritic cells of tumor antigen expressed in apoptotic recombinant canarypox virus-infected dendritic cells. J Immunol 2001;167:1795–802.
16. Yee C, Savage PA, Lee PP, Davis MM, Greenberg PD. Isolation of high avidity melanoma-reactive CTL from heterogeneous populations using peptide-MHC tetramers. J Immunol 1999;162:2227–34.
17. Sallusto F, Mackay CR, Lanzavecchia A. The role of chemokine receptors in primary, effector, and memory immune responses. Annu Rev Immunol 2000;18:593–620.
18. Romero P, Valmori D, Pittet MJ, et al. Antigenicity and immunogenicity of Melan-A/MART-1 derived peptides as targets for tumor reactive CTL in human melanoma. Immunol Rev 2002;188:81–96.
19. Romero P, Dunbar PR, Valmori D, et al. *Ex vivo* staining of metastatic lymph nodes by class I major histocompatibility complex tetramers reveals high numbers of antigen-experienced tumor-specific cytolytic T lymphocytes. J Exp Med 1998;188: 1641–50.
20. Drake DR III, Braciale TJ. Lipid raft integrity affects the efficiency of MHC class I tetramer binding and cell surface TCR arrangement on CD8+ T cells J Immunol 2001;166:7009–13.
21. Skinner PJ, Haase AT. *In situ* tetramer staining. J Immunol Methods 2002;268:29–34.
22. Schrama D, Pedersen LO, Keikavoussi P, et al. Aggregation of antigen-specific T cells at the inoculation site of mature dendritic cells. J Invest Dermatol 2002;119: 1443–8.
23. Saint-Vis B, Vincent J, Vandenabeele S, et al. A novel lysosome-associated membrane glycoprotein, DC-LAMP, induced upon DC maturation, is transiently expressed in MHC class II compartment. Immunity 1998;9:325–36.
24. Dieu MC, Vanbervliet B, Vicari A, et al. Selective recruitment of immature and mature dendritic cells by distinct chemokines expressed in different anatomic sites. J Exp Med 1998;188:373–86.
25. Sozzani S, Luini W, Borsatti A, et al. Receptor expression and responsiveness of human dendritic cells to a defined set of CC and CXC chemokines J Immunol 1997;159:1993–2000.
26. Randolph GJ. Is maturation required for Langerhans cell migration? J Exp Med 2002;196:413–6.
27. Homey B, Dieu-Nosjean MC, Wiesenborn A, et al. Up-regulation of macrophage inflammatory protein-3α/CCL20 and CC chemokine receptor 6 in psoriasis. J Immunol 2000;164:6621–32.
28. Page G, Lebecque S, Miossec P. Anatomic localization of immature and mature dendritic cells in an ectopic lymphoid organ: correlation with selective chemokine expression in rheumatoid synovium. J Immunol 2002;168:5333–41.
29. Kleeff J, Kusama T, Rossi DL, et al. Detection and localization of Mip-3alpha/LARC/Exodus, a macrophage proinflammatory chemokine, and its CCR6 receptor in human pancreatic cancer. Int J Cancer 1999;81:650–7.
30. Fleming MD, Pinkus JL, Alexander SW, et al. Coincident expression of the chemokine receptors CCR6 and CCR7 by pathologic Langerhans cells in Langerhans cell histiocytosis. Blood 2003;101:2473–5.